Talanta xxx (xxxx) xxx

Contents lists available at ScienceDirect

Talanta

journal homepage: www.elsevier.com/locate/talanta

A silver@gold nanoparticle tetrahedron biosensor for multiple pesticides detection based on surface-enhanced Raman scattering

Yuxiao Lu [a,1], Yuting Tan [c,1], Yue Xiao [a], Zhenxi Li [a], Enze Sheng [a,*], Zhihui Dai [a,b,**]

[a] Jiangsu Collaborative Innovation Centre of Biomedical Functional Materials and Jiangsu Key Laboratory of Biofunctional Materials, School of Chemistry and Materials Science, Nanjing Normal University, Nanjing, 210023, People's Republic of China
[b] Nanjing Normal University Center for Analysis and Testing, Nanjing, 210023, People's Republic of China
[c] Department of Pesticide Science, College of Plant Protection, Nanjing Agricultural University, Nanjing, 210095, PR China

ARTICLE INFO

Keywords:
DNA backbone structure
Ag@Au nano-tetrahedron
SERS hotspots
Multiple pesticides detection

ABSTRACT

The detection of multiple pesticides in food and environment is of great importance for human health and safety. In this study, the DNA backbone structure and Ag@Au nanoparticles (NPs) to construct a nano-tetrahedron with the help of the surface-enhanced Raman scattering (SERS) effect by controlling the formation of SERS hotspots and subsequently realized the simultaneous detection of multiple pesticides. The DNA aptamers corresponding to the three pesticides of profenofos, acetamiprid and carbendazim were embedded into the three edges of the DNA tetrahedral skeleton, and the tetrahedral corners were connected to modify the Ag@Au NPs with different Raman signaling molecules. When aptamers recognize the related pesticides, the DNA backbone is deformed. Then Ag@Au NPs approach to each other with SERS hotspots formed and the intensity of the Raman signal increased, realizing the detection of the pesticide content. The biosensor constructed from the SERS substrate with higher sensitivity and lower detection limit (profenofos: 0.0021 ng mL^{-1}; acetamiprid: 0.0046 ng mL^{-1}; carbendazim: 0.0061 ng mL^{-1}). The practicability of this proposed method was verified by adding the recovery rate detection and the accuracy of the method was examined by the analysis of the HPLC-MS method. The proposed SERS biosensor could distinguish and detect three pesticides in food and environmental samples with high sensitivity and low detection limit that can be used in practical applications.

1. Introduction

Since the last century, pesticides have been widely used as chemical reagents to ensure the production of agricultural products. Pesticide residues caused by the excessive use of pesticides and the physical and chemical properties of some pesticides themselves can cause serious environmental problems and endanger human health [1–3]. Therefore, detecting the content of pesticides in environment and agricultural products has become a central issue of scientific research.

As a representative organophosphorus pesticide, profenofos has been widely used in various crops to prevents various pests [4]. Because of its strong toxicity to the human body, this compound seriously affects the learning function of human nerves [5]. To date, profenofos has been gradually replaced by acetamiprid. However, profenofos is difficult to degrade in the environment and its residues are still detected by agricultural products and environmental procedures [6]. Acetamiprid has become one of the most commonly used insecticides. According to the latest research, acetamiprid residues in vegetables can also cause mild acute and harmful effects on humans [7,8]. The residues interfering with the central nervous system of humans and causing many diseases such as Alzheimer's disease, Parkinson's disease, schizophrenia and depression [9]. Carbendazim, the world's most produced fungicide, is often used in combination with profenofos and acetamiprid to prevents crop pests and diseases [10–13]. The latest research in 2018 shows that carbendazim residues may cause endocrine disruption in humans, resulting in genetic toxicity and teratogenic mutagenic effects [14]. Therefore, it is necessary to establish a sensitive, accurate and economical detection method to simultaneously detect the three above-mentioned pesticides.

In recent years, some strategies for simultaneously detecting these

* Corresponding author.
** Corresponding author.
E-mail addresses: 90663@njnu.edu.cn, 90663@njnu.edu.cm (E. Sheng), daizhihuii@njnu.edu.cn (Z. Dai).
[1] The two author contributed equally.

https://doi.org/10.1016/j.talanta.2021.122585
Received 29 April 2021; Received in revised form 31 May 2021; Accepted 1 June 2021
Available online 9 June 2021

three pesticides have been explored. Such as gas chromatography-mass spectrometry (GC-MS), high-performance liquid chromatography (HPLC), and HPLC-MS/MS [4,15–18]. However, these methods still have some shortcomings. Such as low detection sensitivity, cumbersome sample preparation steps, the requirements of large amounts of organic solvents and expensive equipment. These shortcomings limit the wide application of these methods. Therefore, it is necessary to establish a new method with high sensitivity to quantitatively detect the residues of the three pesticides in agricultural products to meet the increasing demand for food monitoring.

SERS uses precious metal nanomaterials (including gold, silver, etc.) and the principle of electromagnetic field enhancement effect to cause the molecules adsorbed on the surface to produce the Raman enhancement effect [19–23]. In general, SERS beacon molecules encode single NP and because of its specificity combined with molecular fingerprints and the sensitivity of the single molecule, it can provide unique optical characteristics for detection. In addition, it can adequately analyze samples in their original state and was unaffected by the sample detection mechanism and background. Thus, SERS has become an important detection tool in many areas [24–27].

However, SERS-encoded single NP typically displays a weak signal and the uncontrollable aggregation of nanoparticles leads to unreproducible SERS signals, which limits their applications. Therefore, controllable nanostructure assembling system formed by a single NP as the coding probe is hot research of the SERS detection for improving the signal strength and the reproducibility, such as dimers, tetrahedrons and satellites [28–30]. Noble metal core-shell nanomaterials have been widely used in SERS due to their unique local surface plasmon resonance (LSPR) characteristics. Ag NPs have an excellent Raman response activity, and the combination of Ag–Au colloid have the properties of the two metals at the same time. Ag@Au NPs could overcome the limitations of the material and morphology of Ag NPs. Thus, the available excitation interval is widened and better Raman response value can be obtained [31,32].

At present, the controllable nanostructure assembling system has been discovered as SERS "tags" for multiple detection. However, they still mainly produce uncontrollable aggregation and cause fluctuations of the SERS intensity when they are bound to a flat substrate. In combination with these works of He et al., Han et al., and Xu et al. [27–29], we found that tetrahedral NPs self-assembled tetrahedronal structures driven by DNA frames may potentially overcome these limitations [33,34]. It was hypothesized that this may be because each DNA frame has six sides and the discrete tetrahedron has the potential for multipath sensing in the liquid phase. In addition, the plasma coupling effect will super-quantitatively track the target and the DNA-self-assembled tetrahedron has a strong SERS signal value. Moreover, because the tetrahedron has high stability under the conditions of high ionic strength, it has the potential of producing reproducible signals in various matrices. Due to the 3D spatial configuration of the tetrahedron, it is possible to better achieve the identification for the target. Considering of the above-mentioned potential advantages of plasma tetrahedron, we prepared a pesticide multi-residue detection platform based on SERS to simultaneously detect profenofos, acetamiprid and carbendazim.

In this study, the synthesized Ag@Au NPs protected by Tween 20 had good dispersibility and good SERS signal response. The DNA-driven self-assembly of an Ag@Au nano-tetrahedron based on SERS technology was established to achieve the simultaneous detection of three pesticides with high sensitivity and stability. As shown in Scheme 1, Ag@Au NPs were synthesized and three types of Raman beacon molecular for labels were used for Ag@Au NPs. The Raman-Ag@Au NPs were linked with three types (G2, G3, and G4) and bare Ag@Au NPs were linked with G1 sulfhydryl-modified oligonucleotide embedded with the pesticide aptamer. The DNA framework was used to drive the self-assembly of Ag@Au NPs that labelled with three types of Raman beacon molecules

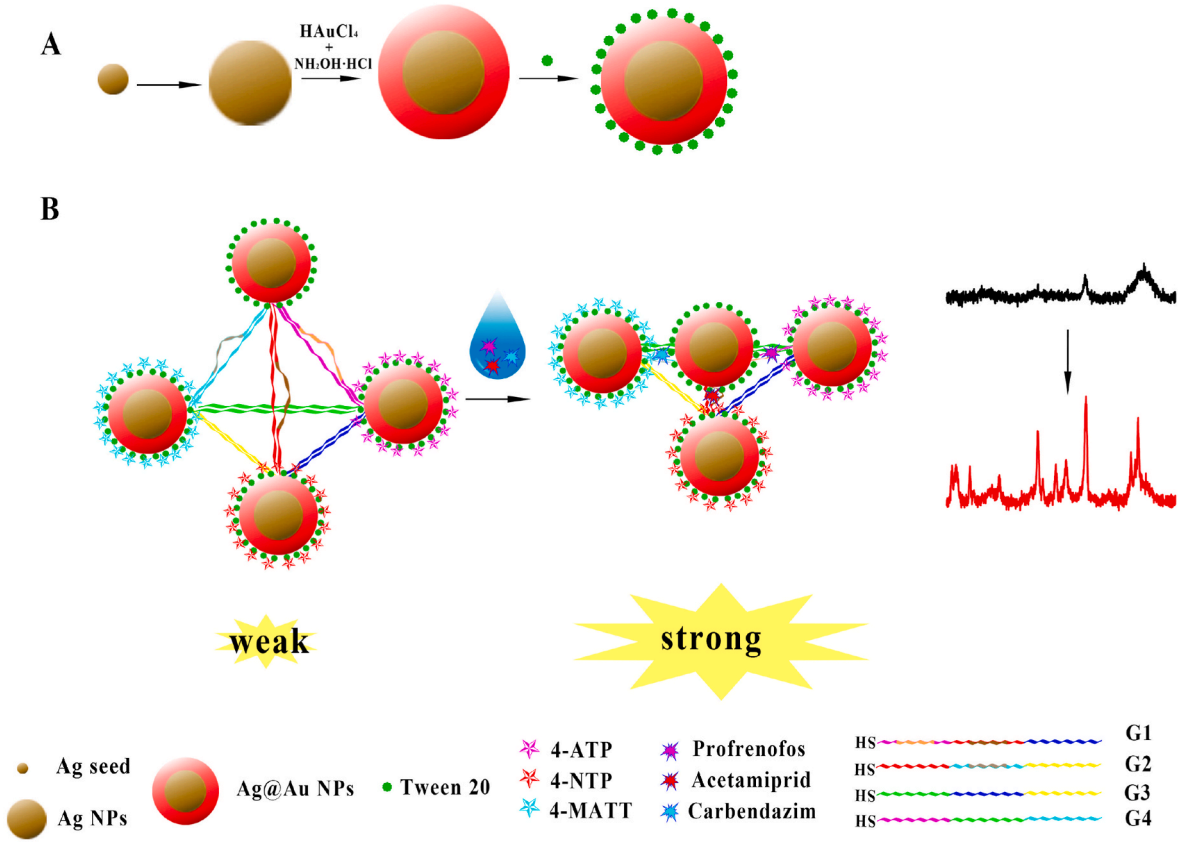

Scheme 1. Schematic illustration of the SERS sensor for detecting multiple analytes based on Ag@Au nano-tetrahedron.

to prepare Ag@Au nano-tetrahedron. Because three sections had specific recognition, the corresponding aptamers in Ag@Au nano-tetrahedron would recognize three pesticides. Consequently, the three-dimensional geometry of the nano-tetrahedron was changed and the gap length was shortened, increasing in the Raman signal. Following the different concentrations of the three pesticides, the SERS signals was linearly amplified. To the best of our knowledge, Ag@Au nano-tetrahedron biosensor for the multiple detection of pesticides based on SERS has not been reported before.

2. Experimental section

2.1. Chemicals and reagents

$AgNO_3$, trisodium citrate, sodium borohydride ($NaBH_4$), chloroauric acid ($HAuCl_4{\cdot}xH_2O$), NH_2OH: HCl, polyvinyl pyrrolidone (PVP), polyoxyethylene sorbitan monolaurate (Tween 20), (Hydroxymethyl) aminomethane (Tris), the standard of the profenofos, acetamiprid and carbendazim, 4-Aminothiophenol (4-ATP), 4-Nitrothiophenol (4-NTP), 4-Methoxybenzyl mercaptan (4-MATT), 50 × Tris-boric acid (TBE) buffer and all other products were purchased from Sigma-Aldrich Chemical Company (USA). Sulfhydryl-modified single-stranded DNA was purchased from Sangon Bio-tech Co., Ltd. (Shanghai, China). All experimental water resistance values were higher than 18 MΩ/cm.

2.2. Apparatus

UV–visible absorption spectrometer (Cary 60 UV–Vis Agilent, USA). Zetasizer nano ZS (UK). Precision pH meter (CTARTER 3100, USA). Transmission electron microscopy (TEM) images were obtained on a JEOL-2100 F apparatus (Japan), the Raman spectra were acquired using a LABRAM HR EVO (HORIBA, France).

2.3. Synthesis of 20 nm Ag NPs

Ag NPs (20 nm) were prepared by seeded growth according to a previously reported method [35]. Firstly, 4 nm Ag seeds protected with citrate were synthesized. Specifically, 20 mL of 1% (w/v) trisodium citrate was added to 75 mL of deionized water in a three-necked flask at 70 °C under stirring and refluxing for 15 min. Next, 1.7 mL of 1% (w/v) $AgNO_3$ and another 2 mL of 0.1% (w/v) $NaBH_4$ were added. The mixture was stirred for 1 h at 70 °C and then cooled to room temperature for later use. Later, 2 mL of 1% (w/v) trisodium citrate was mixed in 80 mL of deionized water in a new flask. The mixture was heated to boiling point and maintained for 15 min. Afterward, 10 mL of 4 nm Ag seeds and 1.7 mL of 1% (w/v) $AgNO_3$ were added. After continuing to boil for 1 h, the mixture was cooled to room temperature. The prepared 20 nm Ag NPs were stored in ultrapure water.

2.4. Preparation of Tween 20 modified Ag@Au NPs

Ag@Au NPs were synthesized by the seeded growth method with modifications and 20 nm Ag NPs were used as seeds [32]. Firstly, 0.5 mL of 20 nm Ag NPs were dispersed in ultrapure water to obtain 15 mL of diluted nanoparticles solution and 154 μL of 100 mM NH_2OH: HCl and 128.7 μL of 10 mM $HAuCl_4$ were added to the solution slowly while gently stirring. After stirring for 45 min, 775 μL of PVP 1 wt% was added to the conjugates and mixed for 20 min. Later, trisodium citrate aqueous solution was added to the mixture to a final concentration of 10 mM, after which, 0.2 wt% Tween 20 was added and the mixture was stirred for 20 min. The resulting Tween 20 modified Ag@Au NPs were centrifuged (three times) at 12000 rpm for 10 min to remove the supernatant and resuspended with Tris-HCl containing 0.2 wt% Tween 20, and then stored in 4 °C for the next use.

2.5. Functionalization of Ag@Au NPs with ssDNA

Briefly, the ssDNA was added to the Tween 20-capped Ag@Au NPs in a ratio of 1:3 and incubated overnight in 0.5 × TBE, 50 mM NaCl. The mixture was then centrifuged (three times) at 12000 rpm for 10 min to remove the supernatants and the deposit was resuspended in Tween 20 (0.2 wt%) with equal volume. Here, four different types of Ag@Au NPs-DNA conjugates were prepared.

2.6. Ag@Au NPs-DNA conjugates modified with Raman beacon molecule

Three types of Raman beacon molecule were used in this work, namely 4-ATP, 4-MATT and 4-NTP. Three types of beacon molecule were dissolved in ethanol under their optimum conditions and added to three different Ag@Au NPs-DNA conjugates. These samples were incubated for 4 h at 27 °C and then centrifuged at 12000 rpm for 10 min and the deposit was resuspended in Tween 20 (0.01 wt%) at an equal volume.

2.7. Synthesis of Ag@Au nano-tetrahedron

A two-step method was used to synthesize Ag@Au nano-tetrahedron according to a previous report with some modifications [29]. First, Ag@Au NPs-DNA conjugates with a hybrid complementary portion were mixed in pairs with an equal volume of Tris buffer (containing 50 mM Na^+, 10 mM K^+, 10 mM Mg^{2+}). The two samples were kept at 90 °C for 5 min and then the temperature was decreased slowly in steam environment until it reached room temperature. Then, the two pairs were mixed in equal volumes and incubated for 24 h at 27 °C. The obtained Ag@Au nano-tetrahedron was stored in 20 mM Tris-HCl containing 0.01 wt% Tween 20.

2.8. Detection of multiple pesticides

To detect profenofos simultaneously, acetamiprid and carbendazim. The SERS sensors were immersed in 20 mM Tris-HCl solution, the standard solution was added to the Tris-HCl solution and the mixture was incubated for 20 min at 37 °C. The SERS spectra of the samples were then acquired. The concentrations of the standard solutions were 1.0×10^{-6}, 1.0×10^{-5}, 1.0×10^{-4}, 1.0×10^{-3}, 1.0×10^{-2}, 1.0×10^{-1}, 1, 10, 100, 1000 and 10000 ng mL^{-1} (profenofos: acetamiprid: carbendazim = 1:1:1).

3. Results and discussion

3.1. Characteristics

The Raman signal can be enhanced by local electromagnetic fields around precious metal nanomaterials. In this study, Ag@Au nano-tetrahedron was used as the SERS substrate material for quantitative detection of pesticides to be tested. As shown in Fig. S1, the Ag seed was spherical and its size was approximately 4 nm (Fig. S1B) with high monodispersity. Fig. S1C shows that the Ag NPs with an average spherical size of 20 nm were uniform. The size of Ag@Au NPs is approximately 30 nm (inset of Fig. 1C). To further verify the core-shell structure of Ag@Au NPs, EDS analysis of Ag@Au NPs is shown in Fig. 1D, displaying the good element distribution of Au (green) and Ag (red) elements.

The maximum absorbance wavelengths of the Ag seeds (Fig. S1A), Ag NPs (Fig. 1A, curve a) and Ag@Au NPs (Fig. 1A, curve b) detected by UV–vis spectra were 400 nm, 398 nm and 575 nm, respectively. The UV–vis absorption peak of the aptamer DNA sequence is at 260 nm (Fig. 1A, curve c). When coupled with Ag@Au NPs, its absorption peak at 575 nm in the absorption spectrum of Ag@Au NPs did not present a red shift (Fig. 1A, curve d), which demonstrated that Ag@Au NPs did not reunite after being modified with DNA. The surface charges of Ag@Au

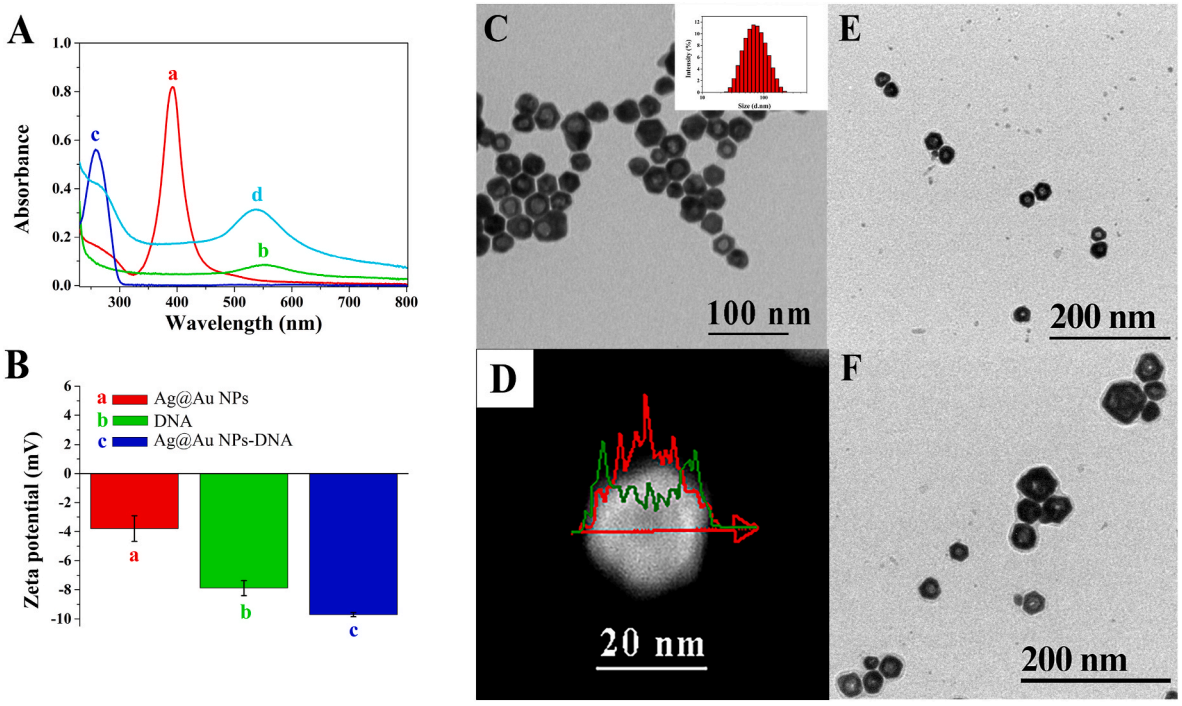

Fig. 1. (A) UV–vis absorption spectrum of 20 nm Ag NPs (curve a), Ag@Au NPs (curve b), DNA (curve c) and Ag@Au NPs coupled with DNA (curve d). (B) Zeta potentials of Ag@Au NPs (column a), DNA (column b), Ag@Au NPs-DNA (column c), (C) TEM images of Ag@Au NPs, (D) EDS analysis of Ag@Au NPs, (E) TEM images of Ag@Au NPs dimers and (F) The TEM images of Ag@Au nano-tetrahedron.

NPs, DNA and Ag@Au NPs after DNA coupling were −3.96, −7.92 and −10.13 mV (Fig. 1B), respectively. Combined with UV–vis spectra, these results could prove that the successful coupling of DNA on the surface of Ag@Au NPs.

Some stabilizers were selected to optimize Ag@Au NPs for good dispersion and stability as shown in Fig. S2. When using trisodium citrate and PVP combined with 0.2 wt% Tween 20 (Fig. S3), Ag@Au NPs have best SERS signals, best dispersion and stability. Therefore, in the

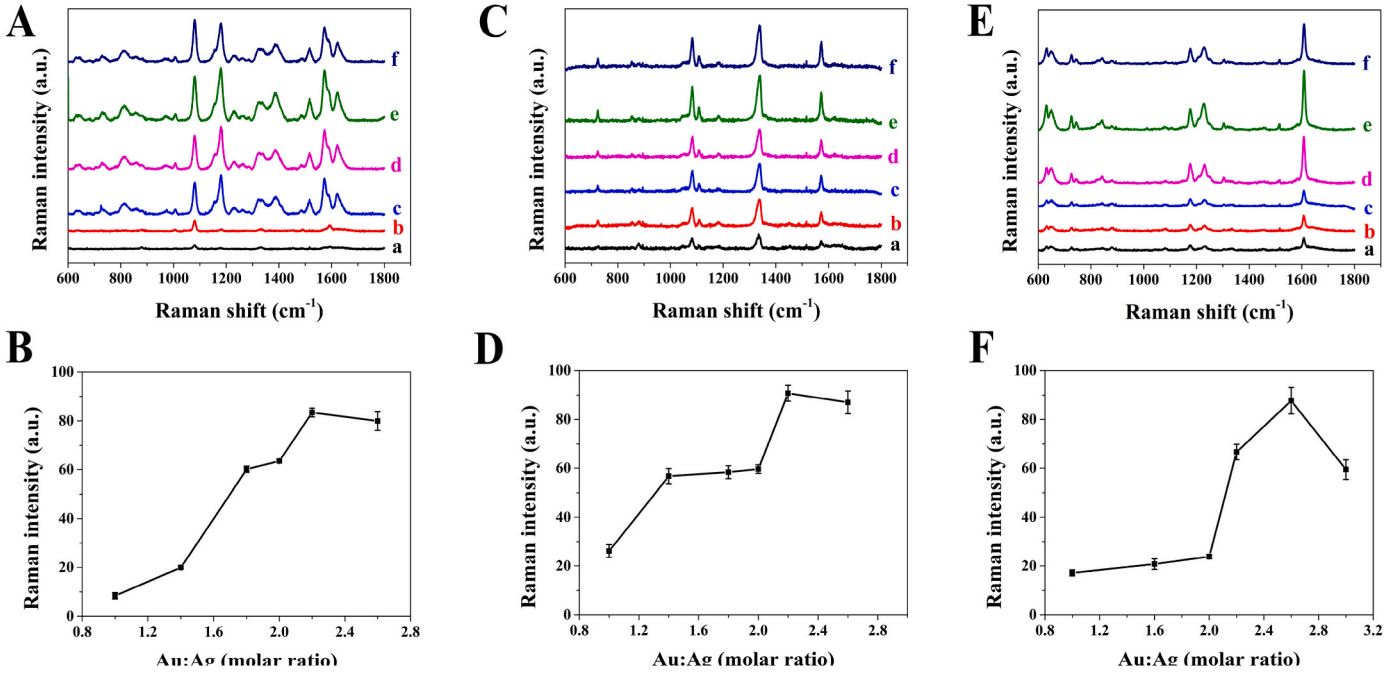

Fig. 2. (A) Strength of SERS-4-ATP-molar ratio of gold/silver (black curve (a): 1.0, red curve (b): 1.4, blue curve (c): 1.8, pink curve (d): 2.0, green curve (e): 2.2 and navy-blue curve (f): 2.6). (B) The corresponding numerical value of the SERS-4-ATP intensity spectra. (C) Strength of SERS-4-NTP-molar ratio of gold/silver (black curve (a): 1.0, red curve (b): 1.4, blue curve (c): 1.8, pink curve (d): 2.0, green curve (e): 2.2 and navy-blue curve (f): 2.6). (D) The corresponding numerical value of the SERS-4-NTP intensity spectra. (E) Strength of SERS-4-MATT-molar ratio of gold/silver (black curve (a): 1.0, red curve (b): 1.6, blue curve (c): 2.0, pink curve (d): 2.2, green curve (e): 2.6 and navy-blue curve (f): 3.0). (F) The corresponding numerical value of the SERS-4-MATT intensity spectra. (For interpretation of the references to colour in this figure legend, the reader is referred to the Web version of this article.)

subsequent preparation of Ag@Au NPs, PVP and Tween-20 were added.

In this study, three types of Raman beacon molecule were used for quantitative analysis, namely 4-ATP, 4-NTP and 4-MATT. To improve the sensitivity and stability, the structure of Ag@Au NPs-labeled beacon molecules was optimized. Most of the signal enhancement of SERS beacon molecules originated from the electromagnetic field generated by the LSPR effect of Ag@Au NPs [23,31,36]. For geometric factors, the thickness of Au shell was largely determined by the strength of LSPR and further influenced intensity of SERS. As shown in Fig. 2A, C and 2E, the SERS intensities of Ag@Au NPs with different shell's thickness enhanced the signals of the three SERS beacon molecules differently. Finally, Ag@Au NPs marked with 4-ATP (Fig. 2B) and 4-NTP (Fig. 2D) when the molar ratio of Au and Ag content was 2.2 and Ag@Au NPs marked with 4-MATT (Fig. 2F) when the molar ratio of Au and Ag content was 2.6 were selected.

After determining the thickness of Ag@Au NPs' shell, the concentrations of three kinds of beacon molecule were also optimized. As shown in Fig. S4, the corresponding peaks of three beacon molecules did not interfere with each other (4-ATP: 1079 cm^{-1}; 4-NTP: 1334 cm^{-1}; 4-MATT: 1609 cm^{-1}), which laid theoretical foundation for the subsequent qualitative and quantitative detection of multiple residues of the three pesticides. When the concentration of 4-ATP was 0.75 μmol L^{-1}, the concentration of 4-NTP was 11 μmol L^{-1} and the concentration of 4-MATT was 3 μmol L^{-1}. The respective beacon molecules labeled by Ag@Au NPs had the highest SERS signal value. Therefore, the beacon molecules with the appropriate Ag@Au NPs shell's thickness and the appropriate concentration above were selected as the raw materials for the subsequent construction of Ag@Au nano-tetrahedron.

In this study, four kinds of complexes formed by Ag@Au NPs and DNA were used to form Ag@Au NPs spatial tetrahedral structure using a two-step method. If single NP aggregates into a cluster, the system would also produce a strong Raman signal, which would adversely affect the sensitivity of the detection result. Fig. 1E shows the TEM of the first step of the self-assembled Ag@Au NPs particle dimers. The photo reveals that Ag@Au NPs dimers were uniformly distributed, the structure was stable and there was no large-scale agglomeration, which was essential for the subsequent construction of Ag@Au NPs spatial tetrahedron. Fig. 1F represents the TEM photograph of the self-assembled Ag@Au nano-tetrahedron. As shown in the Fig. 1F, Ag@Au nano-tetrahedron had uniform distribution, stable structure and good dispersion, which provided a guarantee for the establishment of the subsequent highly sensitive Raman analysis method.

3.2. Feasibility of the assay

To access the feasibility of the constructed Ag@Au nano-tetrahedron system, the DLS diameters of 122.4 nm and 141.8 nm in the absence and presence of profenofos are shown in Fig. 3A. The corresponding maximum absorption peak position of the UV–vis absorption spectrum remained unchanged with Ag@Au nano-tetrahedron states in the absence or presence of profenofos were displayed in Fig. 3B. For the establishment of multi-residue analysis method for profenofos, acetamiprid and carbendazim, the cross-reactivity between analytes was discussed. 50 ng of profenofos, acetamiprid and carbendazim solution were added to the constructed Ag@Au nano-tetrahedron system, respectively. Then, SERS signal detection was carried out. As shown in Fig. 3C (black curve and red curve) compared with the blank sample, the SERS signal of the characteristic peak of 4-ATP at 1079 cm^{-1} increased, while the SERS signal of the characteristic peak of 4-NTP at 1334 cm^{-1} and 4-MATT at 1609 cm^{-1} did not change (Fig. 3D) after the addition of profenofos. The reason for this phenomenon is that Ag@Au nano-tetrahedron in this study that used the specific binding characteristics of nucleic acid aptamers and analytes to distinguished them. The chemical structure of profenofos is very different from the structure of acetamiprid and carbendazim. Therefore, the aptamer of profenofos could only specifically recognize profenofos, but not acetamiprid or carbendazim. And similarly, 50 ng acetamiprid and 50 ng carbendazim were added separately (Fig. 3C: blue curve and rose curve, Fig. 3E and

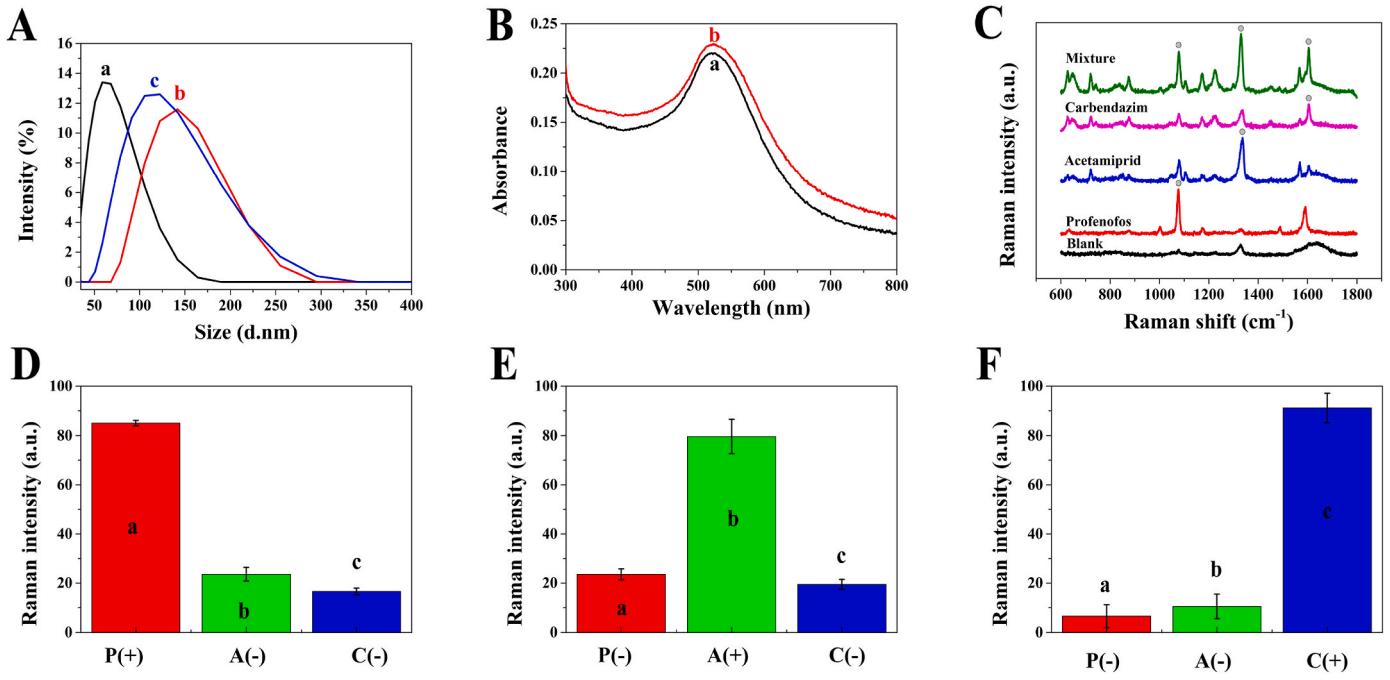

Fig. 3. (A) DLS spectra of Ag@Au NPs (curve a) tetrahedron in the absence (curve b) or presence (curve c) of profenofos (50 ng). (B) UV–vis absorption spectrum of Ag@Au nano-tetrahedron system in the absence (curve a) or presence (curve b) of profenofos. (C) SERS intensity spectra of the cross-reactivity of three pesticides (Black sample: black curve, Profenofos: red curve, Acetamiprid: blue curve, Carbendazim: rose curve and Mixture: green curve). (D) The corresponding numerical value of SERS intensity for profenofos. (E) The corresponding numerical value of SERS intensity for acetamiprid. (F) The corresponding numerical value of SERS intensity for carbendazim (Profenofos: column a, Acetamiprid: column b and Carbendazim: column c). (For interpretation of the references to colour in this figure legend, the reader is referred to the Web version of this article.)

F). Therefore, the cross-reactivity of these pesticides in this study can be neglected.

3.3. Optimization

When pesticide residue testing is conducted, some reagents must be used to extract pesticides from the sample matrix. The three pesticides were soluble in methanol, and methanol at a certain content is conducive to the identification of samples and aptamers. However, high content of methanol would affect the results. In addition, the aptamer is an oligonucleotide sequence or a short polypeptide and the pH value of Tris buffer will affect its activity to a certain extent and even lead to the cleavage and fracture of the aptamer sequence, thus affecting the experimental results. For these reasons, the methanol content and pH of the Tris buffer system were optimized in this study. As displayed in Fig. S5, the Tris buffer contented 2% methanol and pH 7.5 was used for future research.

3.4. Analytical performance

Ag@Au nano-tetrahedron was performed under the optimal conditions to detect a series of samples with varying concentrations of profenofos, acetamiprid and carbendazim. As depicted in Fig. 4, when the pesticide concentrations increased, the SERS intensity would be increased and half maximal inhibitory concentration (IC_{50}) of profenofos was 0.05 ng mL^{-1}, the IC_{10}-IC_{90} was 0.0021–2362 ng mL^{-1} (Fig. 4A). The IC_{50} of acetamiprid was 0.059 ng mL^{-1} and the range was 0.0046–1876 ng mL^{-1} (Fig. 4B), which the IC_{50} of carbendazim was 0.045 ng mL^{-1} and the IC_{10}-IC_{90} was 0.0061–1545 ng mL^{-1} (Fig. 4C). All of the scope of tested met the maximum residue limit (MRL, profenofos: prohibited, acetamiprid: 0.02 mg kg^{-1} and carbendazim: 0.02 mg kg^{-1} in the USA). Moreover, the limit of detection (LOD) of Ag@Au nano-tetrahedron was lower than the existing research results (Table S1) with better sensitivity. The detection time required was also shorter than existing analytical methods. Compared with other methods based on SERS for multiple pesticides analysis qualitatively and quantitatively [37,38], the Ag@Au nano-tetrahedron had lower LOD and less detection time, which showed that the established Ag@Au nanotetrahedron detection method had better detection performance.

3.5. Principle of ultra-sensitive detection

Such a low LOD might be achieved because of the following reasons: 1) The use of aptamers allowed high recognition performance and could identify lower concentrations of analytes [33]; 2) Each DNA frame has six sides, thus the discrete tetrahedron had the potential for multipath sensing in the liquid phase (Scheme 1); 3) Ag@Au nano-tetrahedron was uniformly distributed in the solution and the SERS signal base was low. After the substance to be measured was added into the system, Ag@Au nano-tetrahedron with uniform distribution would be aggregated, thus causing the enhancement of the SERS signals and making the instrument detect the small changes of the SERS signal value [27,29]; 4) The plasma coupling effect super-quantitatively tracks the target and the DNA-self-assembled tetrahedron has a strong SERS signal value [12,26]; 5) Since the three-dimensional spatial configuration of the tetrahedron was very stable, the SERS signal would change accordingly after adding a test sample that would shrink its spatial configuration, which could better achieve target recognition [31].

3.6. The stability of the system

To examine stability of the method, Ag@Au nano-tetrahedron stored for a certain period was used to detect the profenofos, acetamiprid and carbendazim at concentrations of 10, 50, 100 ng mL^{-1}. As displayed in Fig. S6, the detection results of Ag@Au nano-tetrahedron after different storage days (0, 1, 3, 5, 7, 14 d) remained unchanged, which proved that the prepared Ag@Au nano-tetrahedron has good stability.

3.7. Specificity

Aptamer can not only specifically bind to the pesticide to be tested, but also to other compounds with similar structures. This specific binding might cause matters such as false positive detection results, which severely could affect the accuracy and reliability of the detection. Therefore, the cross reactions of these pesticides with similar structures were monitored as dissected in Fig. S7. The pesticides' aptamers used in this work did not cross-react with other pesticides with similar structure.

3.8. Real samples detection

The standard addition recovery rate of the three pesticides detected by Ag@Au nano-tetrahedron was 79.5–98.7% for profenofos, 74.6–100.4% for acetamiprid and 75.6–99.8% for carbendazim, and the relative standard deviation were 3.28–7.56% (profenofos), 2.35–8.69% (acetamiprid) and 2.26–7.86% (carbendazim) as depicted in Table S2. The accuracy and precision of Ag@Au nano-tetrahedron detection met the national standard (NY/T 788-2018). The results shown that Ag@Au nano-tetrahedron was an accurate and feasible method to quickly detect the presence of three pesticides in real samples.

3.9. Comparison with HPLC-MS methods

Analysis of real samples rather than laboratory samples by current methods may be more helpful in demonstrating the reliability of the method [39]. So the results of Ag@Au nano-tetrahedron detection in actual samples were compared with HPLC-MS results (Fig. 5), and these

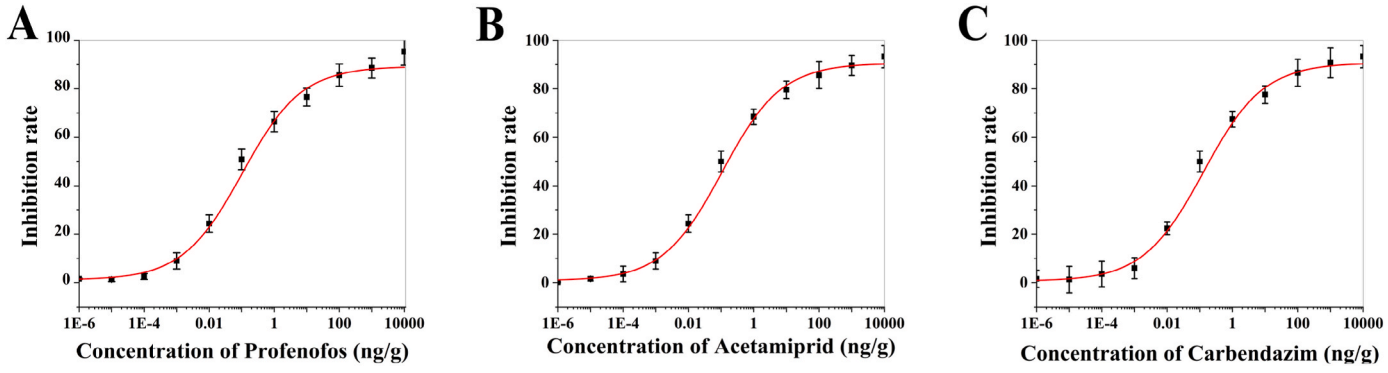

Fig. 4. (A) Standard curve line of Ag@Au nano-tetrahedron of profenofos. (B) Standard curve line of Ag@Au nano-tetrahedron of acetamiprid. (C) Standard curve line of Ag@Au nano-tetrahedron of carbendazim (the concentrations of all pesticides were 1.0×10^{-6}, 1.0×10^{-5}, 1.0×10^{-4}, 1.0×10^{-3}, 1.0×10^{-2}, 1.0×10^{-1}, 1, 10, 100, 1000 and 10000 ng mL^{-1}).

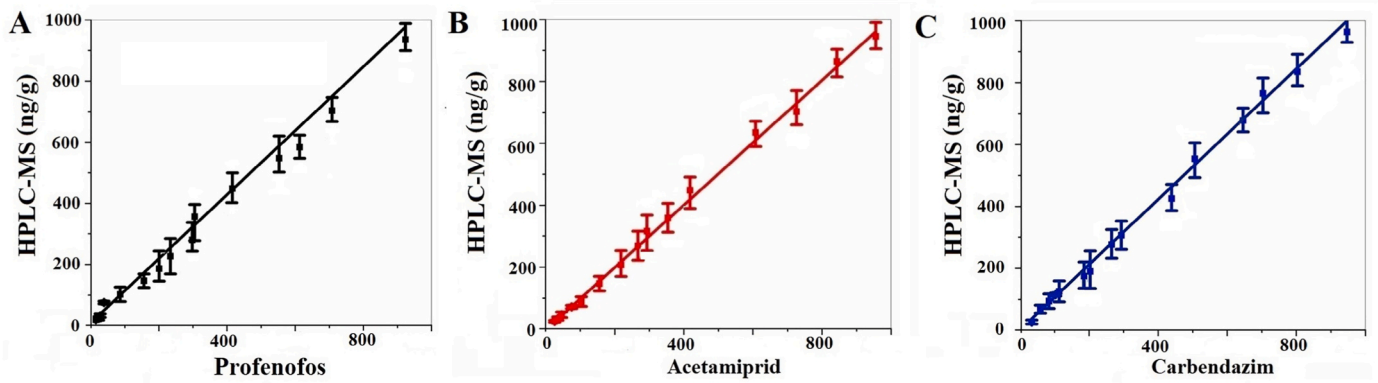

Fig. 5. Correlation between the assay and HPLC-MS for analyses of samples with profenofos (A), acetamiprid (B) and carbendazim (C).

two analytical methods obtained satisfactory favourable correlation (profenofos: $y = 0.9671x + 1.1264$, $R^2 = 0.9947$; acetamiprid: $y = 1.1053x + 0.2463$, $R^2 = 0.9922$; carbendazim: $y = 1.0463x + 0.0681$, $R^2 = 0.9937$). These all illustrated that Ag@Au nano-tetrahedron detection method was exact and dependable in detecting profenofos, acetamiprid and carbendazim residues in environmental and food samples.

4. Conclusion

In this work, three-dimensional nano-tetrahedron of Ag@Au NPs were successfully prepared based on DNA molecular self-assembly. The specific recognition of target and aptamer was used to change the distance between the assembled Ag@Au nano-tetrahedron, forming hot spots of SERS and further resulting in strong Raman enhancement effect. Taking advantage of the spatial configuration and multi-element structure of the tetrahedron, a tetrahedral multiple Raman detection system with three types of beacon molecule was constructed by introducing three-segment nucleic acid aptamers and three beacon molecules into the tetrahedron. The changes in the Raman signals of the three types of beacon molecule correspond to the concentrations of the three target pesticides, thereby realizing the simultaneous detection of the three pesticides of profenofos, acetamiprid and carbendazim. This method exhibited strong identification ability for pesticides in food and environmental samples. The method could realize ultra-sensitive detection with ultra-low LOD level, has good specificity and the detection result is not affected by the disordered aggregation of nanoparticles that more conducive to the practical application of SERS sensing detection technology.

Author contributions

Yuxiao Lu: Writing – original draft, Validation, Formal analysis, Visualization, Software, Yuting Tan: Validation, Formal analysis, Visualization, Software, Yue Xiao: Formal analysis, Zhenxi Li: Formal analysis, Enze Sheng: Conceptualization, Methodology, Formal analysis, Visualization, Software, Writing – original draft, Writing – review & editing, Zhihui Dai: Conceptualization, Methodology, Resources, Writing – original draft, Writing – review & editing, Supervision, Project administration, Funding acquisition.

Declaration of competing interest

The authors declare that they have no known competing financial interests or personal relationships that could have appeared to influence the work reported in this paper.

Acknowledgments

This work was supported by the Natural Science Foundation of China for the project (Nos. 21625502, 21974070).

Appendix A. Supplementary data

Supplementary data to this article can be found online at https://doi.org/10.1016/j.talanta.2021.122585.

Availability of data and material

All data generated or analyzed during this study are included in this published article and its supplementary information files.

References

[1] R. Cai, D. Yang, K.T. Lin, Y.F. Lyu, B.W. Zhu, Z. He, L.L. Zhang, Y. Kitamura, L. P. Qiu, X.G. Chen, Y.L. Zhao, Z. Chen, W.H. Tan, Generalized preparation of two-dimensional quasi-nanosheets via self-assembly of nanoparticles, J. Am. Chem. Soc. 141 (2019) 1725–1734.

[2] Y.P. Zhang, X.T. Liu, S. Qiu, Q.Q. Zhang, W. Tang, H.T. Liu, Y.L. Guo, Y.Q. Ma, X. J. Guo, Y.Q. Liu, A flexible acetylcholinesterase-modified graphene for chiral pesticide sensor, J. Am. Chem. Soc. 141 (2019) 14643–14649.

[3] M. Majdinasab, M. Daneshi, J.L. Marty, Recent developments in non-enzymatic (bio)sensors for detection of pesticide residues: focusing on antibody, aptamer and molecularly imprinted polymer, Talanta (2021) 122397.

[4] X. Ge, P. Zhou, Q. Zhang, Z. Xia, S. Chen, P. Gao, Z. Zhang, L. Gu, S. Guo, Palladium single atoms on TiO_2 as a photocatalytic sensing platform for analyzing the organophosphorus pesticide chlorpyrifos, Angew Chem. Int. Ed. Engl. 59 (2020) 232–236.

[5] X. Yan, Y. Song, X.L. Wu, C.Z. Zhu, X.G. Su, D. Du, Y.H. Lin, Oxidase-mimicking activity of ultrathin MnO_2 nanosheets in colorimetric assay of acetylcholinesterase activity, Nanoscale 9 (2017) 2317–2323.

[6] R.S. Rodriguez, T.L. O'Keefe, C. Froehlich, R.E. Lewis, T.R. Sheldon, C.L. Haynes, Sensing food contaminants: advances in analytical methods and techniques, Anal. Chem. 93 (2021) 23–40.

[7] X. Yan, Y. Song, C.Z. Zhu, H.G. Li, D. Du, X.G. Su, D. Du, Y.H. Lin, MnO_2 nanosheet-carbon dots sensing platform for sensitive detection of organophosphorus pesticides, Anal. Chem. 90 (2018) 2618–2624.

[8] A. Verdian, Apta-nanosensors for detection and quantitative determination of acetamiprid - a pesticide residue in food and environment, Talanta 176 (2018) 456–464.

[9] K.M. Fan, W.K. Kang, S.F. Qu, L. Li, B.H. Qu, L.H. Lu, A label-free and enzyme-free fluorescent aptasensor for sensitive detection of acetamiprid based on AT-rich dsDNA-templated copper nanoparticles, Talanta 197 (2019) 645–652.

[10] A. Wong, A.M. Santos, R.F. Alves, F.C. Vicentini, O. Fatibello-Filho, M. D. Sotomayor, Simultaneous determination of direct yellow 50, tryptophan, carbendazim, and caffeine in environmental and biological fluid samples using graphite pencil electrode modified with palladium nanoparticles, Talanta 222 (2021) 121539.

[11] Y.X. Yang, D.Q. Huo, H.X. Wu, X.F. Wang, J.S. Yang, M.H. Bian, Y. Ma, C.J. Hou, N, P-doped carbon quantum dots as a fluorescent sensing platform for carbendazim detection based on fluorescence resonance energy transfer, Sensor. Actuator. B Chem. 274 (2018) 296–303.

[12] C. Zhai, Y.K. Peng, Y.Y. Li, K.G. Chao, Extraction and identification of mixed pesticides' Raman signal and establishment of their prediction models, J. Raman Spectrosc. 48 (2017) 494–500.

[13] H.J. Yan, L.Q. Liu, N.F. Xu, H. Kuang, C.L. Xu, Development of an immunoassay for carbendazim based on a class-selective monoclonal antibody, Food Agric. Immunol. 26 (2015) 659–670.
[14] R.C.T. Temgoua, U. Bussy, D. Alvarez-Dorta, N. Galland, J. Hémez, C. Thobie-Gautier, I.K. Tonlé, M. Boujtita, Using electrochemistry coupled to high resolution mass spectrometry for the simulation of the environmental degradation of the recalcitrant fungicide carbendazim, Talanta 221 (2021) 121448.
[15] M. Gawel, T. Kiljanek, A. Niewiadowska, S. Semeniuk, M. Goliszek, O. Burek, A. Posyniak, Determination of neonicotinoids and 199 other pesticide residues in honey by liquid and gas chromatography coupled with tandem mass spectrometry, Food Chem. 282 (2019) 36–47.
[16] Y.Y. Zhu, J.J.X. Wu, L.J. Han, X.Y. Wang, W. Li, H.C. Guo, H. Wei, Nanozyme sensor arrays based on heteroatom-doped graphene for detecting pesticides, Anal. Chem. 92 (2020) 7444–7452.
[17] J. Gao, D.W. Chen, Y.F. Zhao, Determination of carbendazim and thiabendazole in wine and beer by ultra high performance liquid chromatography-high resolution mass spectrometry coupled with dispersive micro solid-phase extraction, Chin. J. Chromatogr. 36 (2018) 143–149.
[18] T.T. Hu, C.M. Lu, H. Li, Z.X. Zhang, Y.H. Zhao, J. Li, Determination of eleven organophosphorus pesticide residues in textiles by using HPLC-HRMS, Anal. Sci. 33 (2017) 1027–1032.
[19] M. Fleischmann, P.J. Hendra, A.J. McQuillan, Raman spectra of pyridine adsorbed at a silver electrode, Chem. Phys. Lett. 26 (1974) 163–166.
[20] A. Campion, P. Kambhampati, Surface-enhanced Raman scattering, Chem. Soc. Rev. 27 (1998) 241–250.
[21] M. Moskovits, Surface-enhanced spectroscopy, Rev. Mod. Phys. 57 (1985) 783–826.
[22] M. Moskovits, D.A. Piorek, Brief history of surface-enhanced Raman spectroscopy and the localized surface plasmon dedicated to the memory of Richard Van Duyne (1945-2019), J. Raman Spectrosc. 52 (2021) 279–284.
[23] J.A. Creighton, C.G. Blatchford, M.G. Albrecht, Plasma resonance enhancement of Raman scattering by pyridine adsorbed on silver or gold sol particles of size comparable to the excitation wavelength, J. Chem. Soc., Faraday Trans. 2 (75) (1979) 790–798.
[24] P.L. Stiles, J.A. Dieringer, N.C. Shah, R.P.V. Duyne, Surface-enhanced Raman spectroscopy, Annu. Rev. Anal. Chem. 1 (2008) 601–626.
[25] C.G. Blatchford, J.R. Campbell, J.A. Creighton, Plasma resonance-enhanced Raman scattering by absorbates on gold colloids: the effects of aggregation, Surf. Sci. 120 (1982) 435–455.
[26] S. Schlucker, Surface-enhanced Raman spectroscopy: concepts and chemical applications, Angew Chem. Int. Ed. Engl. 53 (2014) 4756–4795.
[27] Y. Zhu, X.G. Jiang, H.Y. Wang, S.Y. Wang, H. Wang, B. Sun, Y.Y. Su, Y. He, A poly adenine-mediated assembly strategy for designing surface-enhanced resonance Raman scattering substrates in controllable manners, Anal. Chem. 87 (2015) 6631–6638.
[28] J.J. Li, W.J. Wang, H. Zhang, Z.C. Lu, W.X. Wu, M.B. Shu, H.Y. Han, Programmable DNA tweezer-actuated SERS probe for the sensitive detection of AFB1, Anal. Chem. 92 (2020) 4900–4907.
[29] L. Xu, W. Yan, W. Ma, H. Kuang, X. Wu, L. Liu, Y. Zhao, L. Wang, C. Xu, SERS encoded silver pyramids for attomolar detection of multiplexed disease biomarkers, Adv. Mater. 27 (2015) 1706–1711.
[30] M. Muhammad, Q. Huang, A review of aptamer-based SERS biosensors: design strategies and applications, Talanta 227 (2021) 122188.
[31] J.F. Li, Y.J. Zhang, S.Y. Ding, R. Panneerselvam, Z.Q. Tian, Core-shell nanoparticle-enhanced Raman spectroscopy, Chem. Rev. 117 (2017) 5002–5069.
[32] G.V.P. Kumar, S. Shruthi, B. Vibha, B.A.A. Reddy, T.K. Kundu, C. Narayana, Hot spots in Ag core-Au shell nanoparticles potent for surface-enhanced Raman scattering studies of biomolecules, J. Phys. Chem. C 111 (2007) 4388–4392.
[33] N.C. Seeman, DNA in a material world, Nature 421 (6921) (2003) 427–431.
[34] J. Nangreave, D.R. Han, Y. Liu, H. Yan, DNA origami: a history and current perspective, Curr. Opin. Chem. Biol. 14 (2010) 608–615.
[35] Y. Wan, Z. Guo, X. Jiang, K. Fang, X. Lu, Y. Zhang, N. Gu, Quasi-spherical silver nanoparticles: aqueous synthesis and size control by the seed-mediated Lee-Meisel method, J. Colloid Interface Sci. 394 (2013) 263–268.
[36] S.Y. Ding, E.M. You, Z.Q. Tian, M. Moskovits, Electromagnetic theories of surface-enhanced Raman spectroscopy, Chem. Soc. Rev. 46 (2017) 4042–4076.
[37] S.M. Zou, M.J. Hou, J.H. Li, L.W. Ma, Z.J. Zhang, Semi-quantitative analysis of multiple chemical mixtures in solution at trace level by surface enhanced Raman scattering, Sci. Rep. 7 (2017) 6186–6194.
[38] M.J. Hou, Y. Huang, L.W. Ma, Z.J. Zhang, Quantitative analysis of single and mix food antiseptics basing on SERS spectra with PLSR method, Nano. Res. Lett. 11 (2016) 296–303.
[39] S.M. Zou, L.W. Ma, J.H. Li, Z. Xie, D.L. Zhao, Y.H. Ling, Z.J. Zhang, Quantification of trace chemicals in unknown complex systems by SERS, Talanta 186 (2018) 452–458.